Sensors and Actuators Reports 9 (2025) 100340

Contents lists available at ScienceDirect

Sensors and Actuators Reports

journal homepage: www.sciencedirect.com/journal/sensors-and-actuators-reports

Extended gate organic field effect transistor for calcium ion sensing towards biomedical applications

F. A. Viola [a], D. Hatami [a,b], F. Mariani [c], I. Gualandi [c], F. Terranova [d], E. Scavetta [c], A. Bonfiglio [b,*], A. Spanu [b]

[a] Department of Electrical and Electronic Engineering, University of Cagliari, via Marengo, Cagliari 09123, Italy
[b] University School for Advanced Studies (IUSS), Piazza della Vittoria 15, Pavia 27100, Italy
[c] Department of Industrial Chemistry "Toso Montanari", University of Bologna, Via Piero Gobetti 85, Bologna, Italy
[d] Department of Informatics, Bioengineering, Robotics and Systems Engineering, University of Genova, Genova, Italy

ARTICLE INFO

Keywords:
Extended gate OFET (ExG-OFET)
Free calcium ion detection
Ion sensing
Supernerstian sensitivity
Liquid processable ion-selective membranes

ABSTRACT

The measurement of calcium ions (Ca^{2+}) concentration is crucial for several biomedical applications because it plays a key role in various physiological processes, including cellular signalling, muscle contraction, bone metabolism, and the release of neurotransmitters. In this paper, we propose an innovative flexible sensor based on an Extended Gate Organic Field Effect Transistor (ExG-OFET) coupled with a liquid-processable ion-selective membrane. This novel approach enables highly sensitive (exceeding 60 mV dec^{-1}) and selective ion detection, with a limit of detection in the low μM range, outperforming conventional ion-sensitive electrodes (ISEs) due to the intrinsic electronic amplification of the transistor architecture.

Moreover, the simple fabrication process and the use of flexible, cost-effective materials, make this device a versatile, low-cost solution for a wide range of biomedical applications, from in vitro electrophysiology to epidermal electronics. This study highlights the potential of the ExG-OFET platform as a promising alternative to traditional ion detection systems.

1. Introduction

The ability to determine the electrolyte composition of biofluids is relevant for several biomedical applications [1]. Among the different ions, calcium (Ca^{2+}) plays a particularly crucial role, as it is involved in several physiological mechanisms, ranging from cellular signalling and muscle contraction to bone metabolism and neurotransmitter release [2–4]. Indeed, calcium ions are vital for the transmission of electrical signals in both neuronal and muscle cells, acting as secondary messengers in processes such as neurotransmitter release and excitation-contraction coupling [5,6].

Ca^{2+} is important for maintaining cellular resting potential and regulates several stages of the cellular life cycle [7,8]. In the nervous system, calcium ions are fundamental as they participate in the transmission of the depolarizing signal and contribute to synaptic activity: for instance, it has been demonstrated that alterations in extracellular calcium concentrations significantly impact calcium-dependent signalling pathways, highlighting the critical role of calcium in maintaining neuronal function [9,10]. Calcium ions also play a central role in excitation-contraction coupling in both cardiac and vascular smooth muscles, where they functionally interact with other cations, such as sodium (Na^{+}), potassium (K^{+}), and magnesium (Mg^{2+}) [11]. Similarly, Ca^{2+} regulates the contractile function of skeletal muscles, acting on ATP provision [12]. From a physiological perspective, it is also a critical marker for bone health, influencing both bone formation and function [13]. Furthermore, calcium distribution and concentration in various biofluids, including blood, interstitial fluid, urine, sweat, and intra/-extracellular fluids, could be used as a relevant biomarker, thus further emphasizing its significance in human health [14–16]. For instance, hypocalcemia can indicate conditions such as vitamin D deficiency, hypoparathyroidism, or resistance to parathyroid hormone [17]. Conversely, hypercalcemia is often associated with primary hyperparathyroidism or malignancy [18]. In clinical practice, approximately half of the total serum calcium ion exists in its free form, while the remainder is predominantly bound to proteins such as albumin. Since calcium ions represent the biologically active form, measuring their concentration provides a more accurate assessment of calcium status than total serum calcium levels [19].

* Corresponding author.
E-mail address: annalisa.bonfiglio@iusspavia.it (A. Bonfiglio).

https://doi.org/10.1016/j.snr.2025.100340
Received 24 February 2025; Received in revised form 20 May 2025; Accepted 21 May 2025
Available online 21 May 2025

The standard tools for calcium ion sensing are (i) ion-sensitive electrodes (ISEs) and (ii) photometric systems. The core component of an ISE is the ion-selective membrane, which generates a potential difference proportional to the logarithm of the target ion's activity. This potential difference arises from the equilibrium distribution of the target ion between the membrane and the analysed solution [20,21]. Li et al. [22] proposed a Ca^{2+} ion-sensitive electrode with a sensitivity of 30 mV dec^{-1} and a limit of detection (LOD) of 1.6×10^{-7} M. Nyein et al. [23] reported a Ca^{2+}-ISE, enabling real-time, non-invasive monitoring of Ca^{2+} in the mM range concentration in multiple body fluids and a sensitivity of 35 mV dec^{-1}, with good selectivity toward pH variations.

The performance of ISEs is dependent on the stability and specificity of the membrane, which may contain ionophores to impart selectivity [24]. Despite their widespread use, ISEs still face several challenges. They usually have a large form factor and, as passive elements, ISEs do not provide a direct amplification of the signal, meaning that they typically require integration with additional instrumentation to amplify and convert the measured potential into usable data output [25,26]. Furthermore, their sensitivity is inherently limited by the theoretical slope predicted by the Nernst equation, which constrains their ability to achieve higher detection performance.

Unlike ISEs, photometric systems typically measure the intensity of light absorbed or emitted directly by ions or by chemical compounds derived from them [27,28]. These systems offer high sensitivity and stability but are less suited for continuous or rapid analyses due to their reliance on larger sample volumes, complex experimental setups and luminophor degeneration, which leads to signal attenuation with time [29].

Field effect devices have also been investigated for ion sensing [30], with the interest being sparked by the introduction of the ion-sensitive field effect transistor (ISFET) [31]. Unlike ISEs and photometric systems, FETs provide active signal amplification, enabling a more efficient transduction mechanism for biosensing. Moreover, they can be easily miniaturized and integrated into wearable, compact systems [32].

In ISFETs, the gate region is typically covered with a specific ion-selective membrane that can lead to surface potential variation at the gate region when exposed to changes in ion concentration in the surrounding solution, thereby modulating the threshold voltage (V_{TH}) and thus modifying the conductivity of the channel [32].

The ability to detect ions by controlling the electric field has been recently extended with the use of organic semiconductors, such as Electrolyte Gated Organic Transistors (EGOTs). These devices have gained significant attention as promising transducers in bioelectronics due to their low-voltage operation, and the ability of permeable/impermeable organic semiconductors to detect ionic species when exposed in aqueous environments [33]. To improve the selectivity, the integration of the organic semiconductor with ion-selective membranes has been also widely studied [34,35].

However, one of the major challenges with EGOTs for biosensing applications is their low operational stability. Specifically, the output current can significantly drift during operation due to well-known unwanted effects such as swelling of the active layer, which limits the long-term reliability and performance of the device [36,37]. This issue is particularly critical for applications in biological systems, where stable performance is crucial for accurate measurements.

One promising strategy to address these challenges involves the use of extended gate and floating gate architectures. This approach is based on decoupling the sensing area from the active organic semiconductor channel and aims to minimize the direct influence of environmental factors on the organic semiconductor, thereby improving stability [38,39]. Indeed, these architectures have been shown to enhance the stability and reliability of transistor biosensors while maintaining a sensitive and selective detection interface even in complex applications such as in vitro electrophysiology [40,41]. Moreover, the integration of an ion-selective membrane with the extended gate of a field effect transistor enables signal amplification by converting the variations in ionic concentration into electrical signals. The potential drop at the interface between the membrane and the solution modulates the threshold voltage of the FET, leading to changes in the output current proportional to the transistor's transconductance (which can be considered an amplification factor) [42].

In this paper, we present a novel calcium ion sensor based on a low-voltage extended gate organic transistor (ExG-OFET) that can be fabricated onto cost-effective plastic substrates using low-resolution lithography and solution-processable materials. The device is coupled with a polymeric Ca^{2+}-selective membrane combined with an all-solid-state ion-to-electron transducer, forming a solid contact ion-selective gate electrode. This approach offers interesting improvements over standard potentiometric techniques due to the convenient fabrication approach and materials, and the intrinsic electrical amplification given by the peculiar transistor's structure. To the best of our knowledge, no similar approaches have been reported so far for calcium detection.

The sensing capabilities of this device show promising results in terms of sensitivity (exceeding 60 mV dec^{-1}, well above the typical values reported for standalone Ca^{2+} ISEs [22,23]), as well as selectivity towards common interferents, linear response, and limit of detection in the low μM range.

2. Experimental section

Chemicals and Buffers. Potassium nitrate, sodium hydroxide, phosphoric acid, calcium nitrate, sodium polystyrene sulfonate (NaPSS), 3,4-ethylenedioxythiophene (EDOT), N,N-Dicyclohexyl-N′,N′-dioctadecyl-3-oxapentanediamide (ETH5234, Calcium Ionophore IV), ortho-nitrophenyloctyl ether (o-NPOE) and anhydrous inhibitor-free tetrahydrofuran (THF) were purchased from Merck. High Molecular Weight polyvinyl chloride (HMW-PVC) was obtained from Fluka. Potassium tetrakis(4-chlorophenyl)borate was acquired from Alfa Aesar. All chemicals used were of reagent grade or higher. The buffer for the preliminary characterization of the membrane was 0.1 M KNO_3, while the buffer employed for the characterization of the organic sensor was the same but with the addition of 10 mM of KCl (to stabilize it due to the use of a Ag/AgCl pseudo reference electrode). As for the pH interference measurements, the buffer employed contained 0.1 M KNO_3 and 10 mM H_3PO_4 and its pH was adjusted using 1 M KOH. As for the sodium, magnesium and Glucose interference measurements, it has been used $NaNO_3$, $Mg(NO_3)_2$, and glucose stock solutions, respectively, and the characterizations have been performed in a buffer containing 0.1 M KNO_3 and 10 mM of KCl.

Apparatus. All electrochemical experiments were carried out with an Autolab PGSTAT204 potentiostat. Potential-controlled and open-circuit potential measurements were carried out with an aqueous saturated calomel reference electrode (SCE) and, when needed, using a Pt wire as a counter-electrode (CE). All solution-based pH measurements were conducted using a combined glass electrode (Amel 411/CGG/12) connected to a pH meter (Amel instruments 338).

The characterization of both the transistors and sensors was performed using a Keithley 2612B controlled by a custom Python software.

Devices fabrication. To fabricate the sensors, polyethylene terephthalate (PET) with a thickness of 175 μm was selected as the substrate. A thin film of aluminum (Al) was deposited onto the substrate via thermal evaporation. Photolithography was employed to define the aluminum gate pattern, while chemical etching (with hydrofluoric acid) was utilized to remove aluminum in unprotected areas. The dielectric layer comprises a 6 nm-thick Al_2O_3 layer that was grown by mild oxygen plasma treatment and 200 nm-thick Parylene C film. After the dielectric layer deposition, gold source and drain electrodes were patterned on the Parylene C film using the same standard photolithographic process used for the floating gate fabrication. For all the devices, 3,6-diketopyrrolopyrrole-alt-5,5-(2,5-di(thien-2-yl)thieno [3,2-b]thiophene) (Sigma-Aldrich) was used as organic semiconductor. A solution of 1 wt. % of DPP-TTT in dichlorobenzene was drop-casted onto the channel area.

Functionalization of the gate electrode. Au surfaces were first modified through the electrochemical deposition of a PEDOT:PSS film. This was done in a 3-electrode cell containing an aqueous solution made of 10 mM EDOT and 0.1 mM NaPSS upon application of a linear scan of electrochemical potential (E) from 0 to 1.1 V vs SCE at 100 mV s-1, for 5 or 10 deposition cycles. Cyclic voltammetry was selected as it allows periodic monomer replenishment and offers fine control over film growth dynamics, resulting in a homogeneous coating, well suited for integration with ion-selective membranes. This method has been extensively optimized by our group in previous studies [43,44] to ensure uniform, reproducible films while minimizing overoxidation. The Ca^{2+}-selective cocktail was prepared as follows: 2.9 mg of HMW-PVC and 9 µL of o-NPOE were mixed in 170 µL of anhydrous inhibitor-free THF; then, 2 µL of potassium tetrakis(4-chlorophenyl)borate solution in THF (25 mg mL^{-1}) and 15 µL of ETH5234 solution in THF (20 mg mL^{-1}) were added. The resulting ionophore:lipophilic salt molar ratio is 3.7. The ion-selective cocktail was stored at 4 °C inside a vial. For membrane formation, 3 or 5 µL of the cocktail were drop-cast on the electrodes surface and allowed to dry at room temperature for a couple of minutes following THF evaporation. Then, the electrodes were kept at 70 °C for 15 min. The resulting membranes were subjected to a conditioning step in 10 mM $Ca(NO_3)_2$ for 5 days before use.

3. Results and discussion

3.1. Extended gate transistor characterization

The electrical characterization of the proposed p-type ExG-OFETs (the structure of the devices used for the characterization, which are in a bottom-gate/bottom-contact configuration, is shown in Fig. 1a) is summarized below, presenting data averaged over 18 devices using a 3,6-diketopyrrolopyrrole-alt-5,5-(2,5-di(thien-2-yl)thieno[3,2-b]thiophene) (DPP-TTT) based organic semiconductor. In order to evaluate the performance of the transistors (separately from their characterization as sensors), the devices have been characterized by directly biasing the extended gate. As reported elsewhere, the capacitance of the employed dielectric approaches the value of 13.5 nF/cm^2, ensuring appropriate low-voltage device operation [45]. Statistical analysis revealed a threshold voltage of 4.5 ± 1.5 V and a hole mobility (μ_p) of (1 ± 0.34) × 10^{-2} cm^2/Vs. The extracted hole mobility values are consistent with reported benchmarks for similar DPP-TTT based low voltage OFETs, confirming the suitability of the fabrication process for reliable performance [46]. The ExG-OFET operates at low voltage, with clear field-effect modulation, and it shows almost ideal output and transfer curves, with a negligible hysteresis, as it can be seen from the characteristic curves shown in Fig. 1b and 1c.

3.2. Ion-selective membrane characterization

The sensing element of the ExG-OFET is an Au gate electrode coated with an electroactive poly(3,4-ethylenedioxythiophene):polystyrene sulfonate (PEDOT:PSS) film and a polymeric Ca^{2+}-selective membrane. PEDOT:PSS was chosen to form a solid contact with high redox capacitance, which is known to assist efficient ion-to-electron transduction and to improve the potential stability of the membrane-based electrode [47,48]. Compared to other electroactive polymers, it benefits from tunable interfacial properties: for instance, it has been recently reported that the thickness and substrate interactions of PEDOT:PSS layers significantly influence the equilibration behavior and potential stability of solid-contact ISEs [49]. Moreover, PEDOT:PSS derivatives can suppress CO_2 interference [50]. The functionalization procedure was optimized in terms of (i) number of deposition cycles employed during PEDOT:PSS electrodeposition and (ii) area of the Au electrode. The potentiometric response to Ca^{2+} of all modified electrodes was then acquired using a 2-electrode cell with a bulk SCE reference electrode and the resulting analytical parameters were compared. Initially, 3 × 3 mm^2 Au electrodes were coated with PEDOT:PSS upon application of 5 or 10 deposition cycles, with the following drop-cast of 3 µL of ion-selective cocktail. In both cases, the average sensitivity accounted for 19 mV dec^{-1} (N = 2 for each set of electrodes), while a slightly improved linearity of the calibration curve (R^2) was found in the case of 5 deposition cycles, which was selected for further studies. In particular, repeatability was thoroughly investigated to define the linear response range (from 1 × 10^{-4} to 2 × 10^{-2} M) and the limit of detection ((3.9 ± 0.2) × 10^{-5} M). Afterwards, the electrode area was considered. 4 × 4 mm^2 modified electrodes were prepared using 5 deposition cycles and a

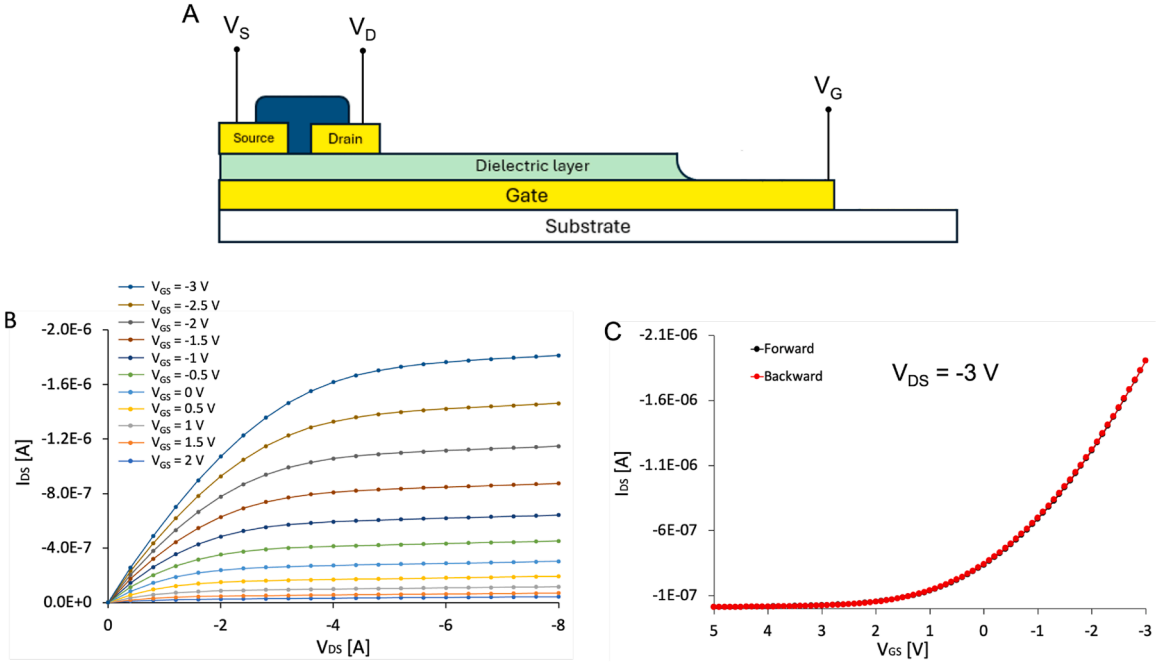

Fig. 1. A) Structure of the ExG-OFET used for the electrical characterization. Output (B) and transfer (C) characteristic of one of the low-voltage ExG-OFETs used in this paper.

proportionally higher drop-cast volume of 5 µL. In this case, we observed significant improvement in sensitivity (23 mV dec^{-1}, $N = 2$), intercept variability, as well as R^2, at the expense of a slightly higher response time. Fig. 2 shows the potentiometric response of a modified electrode following the optimized functionalization protocol. Except for the first addition, where Ca^{2+} concentration was below the LOD, stepwise increments of the electrochemical potential were recorded and could be correlated with the logarithm of Ca^{2+}concentration, in accordance with the Nernst equation. The drift rate is 0.2 mV/min in 0.1 M KNO_3 and 0.090 mV/min in the presence of 500 µM Ca^{2+}. The average response time, calculated as the time required for three potentiometric sensors to reach 90 % of the final signal after a Ca^{2+} addition in the middle of the calibration curve, is 7 ± 3 s. The corresponding calibration curve shows a sensitivity of 22.8 mV dec^{-1} and an intercept of 73 mV.

3.3. Sensor characterization

The structure of the sensor is depicted in Fig. 3a: it consists of two physically separated components, (i) the low-voltage ExG-OFET and (ii) an element comprising a gold layer coated by a PEDOT:PSS film and an ion-selective membrane. The extended gate of the device was physically connected to the gold surface using a thin copper wire, allowing signal transduction without contact between the active layer (i.e., the organic semiconductor) and the analyte solution. The ion-selective membrane, deposited on a PEDOT:PSS-modified gold substrate, is immersed in a calcium-containing aqueous solution together with a custom-made Ag/AgCl reference electrode. With this setup the transistor is effectively gated through the solution. The ExG-OFET based sensor operates by the modulation of the carrier concentration in the DPP-DTT semiconducting channel induced by the variation of the surface potential of the extended gate. Specifically, the increase of Ca^{2+} concentration leads to a more negative threshold voltage, reducing hole accumulation in the p-type ExG-OFET and subsequently lowering the output current intensity (I_{DS}). This configuration allows for real-time, label-free detection of calcium ions with high selectivity and low noise, while preventing the organic semiconductor layer from the contact with the solution.

The output current was measured in real time upon the increase of Ca^{2+} concentration (in the range 0.1 µM - 18.6 mM). As shown in Fig. 3b, the sensor exhibited a clear and reproducible current variation consistent with the expected transduction mechanism, where changes in ion concentration modulate the potential at the gate interface, resulting in corresponding modulation of the channel current. Moreover, the sensor showed remarkable stability in terms of drift current (with values ranging from a few nA/min to a few hundreds pA/min), as well as low noise levels (which is as low as 0.2 nA_{RMS}), highlighting the stability and reliability of the proposed configuration. The obtained response time was 3 ± 1 s for the ExG-OFET based sensor, significantly faster than the 7 s measured for the potentiometric transducer under the same conditions. From this measurement, the variations of the device threshold voltage are extrapolated, allowing to derive a sensitivity of 56 mV dec^{-1}, thus exceeding the limit imposed by Nernst equation and demonstrating the amplification ability of the transistor. To evaluate device-to-device repeatability, 9 different measurements have been taken with three different ExG-OFETs. The statistics of the calibration curve, with the mean and the standard deviation values, is shown in Fig. 3c. From this graph we extrapolated a sensitivity of 63 mV dec^{-1}, which not only exceeds the theoretical Nernstian limit, but also is nearly three times higher than that obtained by the characterization of the standalone membrane in this study (i.e., 23 mv dec^{-1}) operating in a potentiometric configuration under similar conditions, and approximately double the sensitivity typically reported in literature for other ion-selective membranes with analogous configurations [22,23], thus demonstrating the amplification ability of the transistor. Indeed, this significant enhancement can be attributed to the low noise of the system and the direct electronic amplification provided by the ExG-OFET architecture, where the transistor acts as an active transducer that not only detects the ions-induced potential variations at the gate, but also amplifies them directly in the output signal.

To assess the response of the sensor to pH variability (which represent a common interference due to the presence of PEDOT:PSS in the structure of the solid contact ion-selective electrode [51]), the output current was monitored upon variation of pH in the range 5.5 - 7.5. As can be appreciated in Fig. 4a, the sensor is not influenced by pH variations. In fact, apart from a rather limited drift (5.2 nA/min), the current does not appreciably vary upon the variation of the pH while it dramatically changes when the Ca^{2+} concentration is varied at the end of the measurement.

In addition to pH, further interference assessments were performed

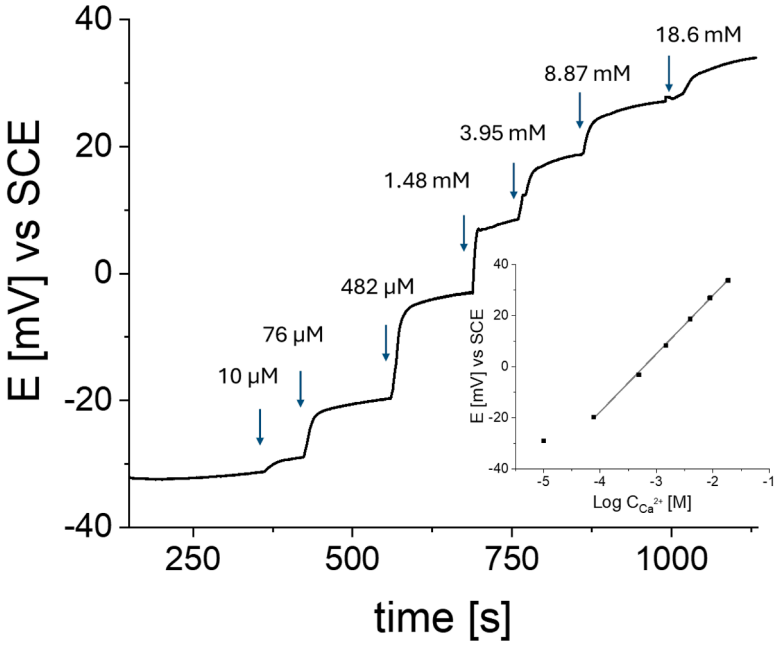

Fig. 2. Characterization of the Ca^{2+}-sensitive membrane. Potentiometric response of an electrode modified with 5 deposition cycles of PEDOT:PSS and the drop-cast ion-selective membrane (active area 16 mm^2) during increasing $Ca(NO_3)_2$ additions to 0.1 M KNO_3 (indicated by blue arrows). Inset: calibration curve, R^2 0.999.

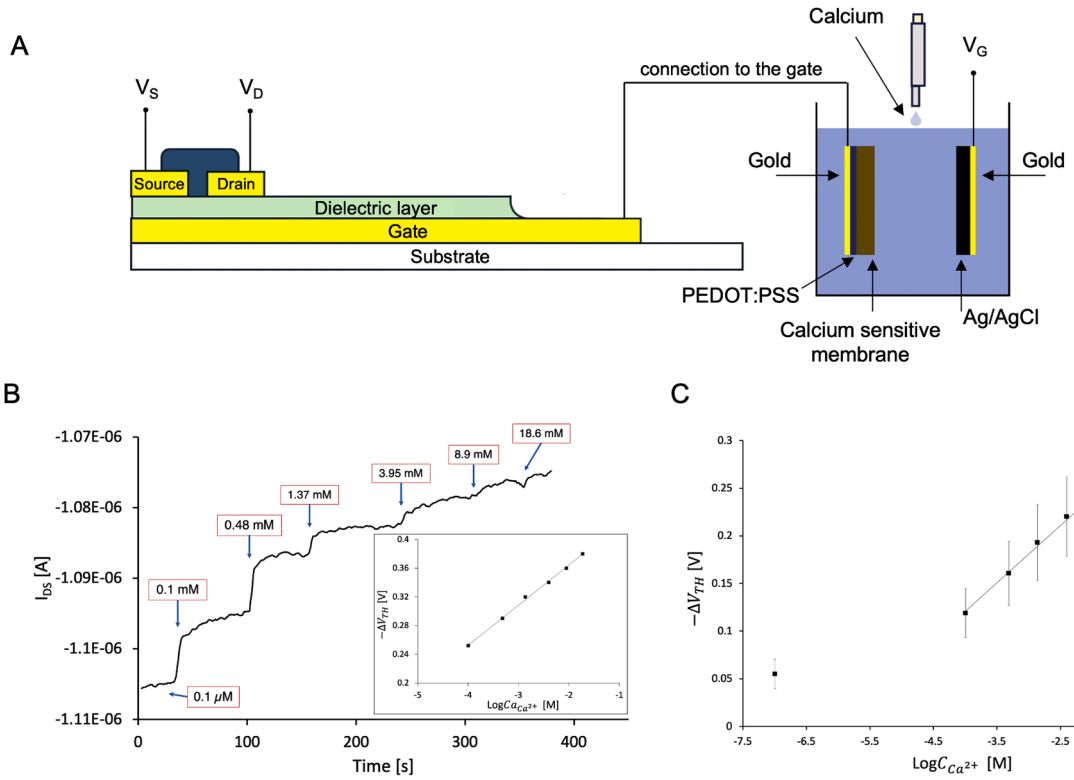

Fig. 3. Sensor characterization. A) Structure of the ExG-OFET-based Ca^{2+} sensor. B) I_{DS} VS Time of one of the sensors used in this paper upon pCa^{2+} variations. For all the experiments, the devices have been gated using a pulsed gate-source voltage V_{GS} (effective voltage −2.5 V) and a constant drain-source voltage V_{DS}=−2.5 V. Inset: calibration curve, sensitivity 56 mV dec^{-1}, R^2 0.998. c) Statistic on 9 different measurements done with 3 different devices and the same Ca^{2+}-sensitive membrane (sensitivity 63 mV dec^{-1}, R^2 0.995).

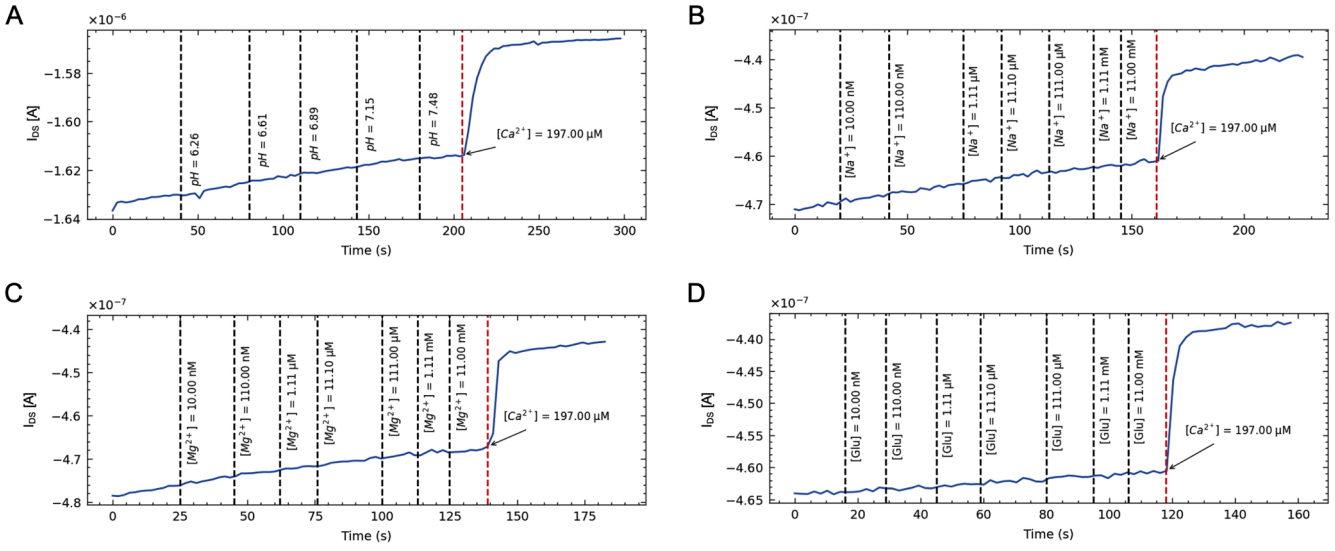

Fig. 4. Effect of interferents. A) I_{DS} variation recorded over time upon pH variations in the electrolyte solution. The last step is relative to the addition of a high calcium concentration. B) I_{DS} variation recorded over time upon sodium variations in the electrolyte solution. The last step is relative to the addition of a high calcium concentration. C) I_{DS} variation recorded over time upon magnesium variations in the electrolyte solution. The last step is relative to the addition of a high calcium concentration. D) I_{DS} variation recorded over time upon glucose variations in the electrolyte solution. The last step is relative to the addition of a high calcium concentration.

to better evaluate the selectivity of the sensor: specifically, sodium, magnesium and glucose at increasing concentrations were tested, which are relevant species often co-present in biological fluids. Starting from the same buffer conditions used for calcium detection, volumes ranging from 2 μL to 200 μL of concentrated stock solutions were added to the test solution to incrementally raise the concentration of each interferent from 10 nM up to 11 mM. As illustrated in Fig. 4b-d, the output current remained unaffected by these additions, indicating a negligible response to the tested interferents. This behavior demonstrates the sensor's robustness and high selectivity toward Ca^{2+} even in the presence of

potential interferents at concentrations several orders of magnitude higher than the target ion, under conditions relevant to biomedical analysis.

Furthermore, the limit of detection of the ExG-OFET-based calcium sensor was evaluated through four independent calibration experiments. The LOD was determined as the calcium ion concentration corresponding to the intersection of the linear regression line with the voltage equivalent of three times the noise level. The extracted LOD values are in the low micromolar range: 1.2 μM, 2.0 μM, 1.8 μM, and 1.5 μM, yielding a mean LOD of 1.6 ± 0.3 μM. These values represent an improvement compared to the standalone ion-selective membrane evaluated under the same conditions, which exhibited a LOD of more than one order of magnitude higher (i.e., $(3.9 \pm 0.2) \times 10^{-5}$ M). This enhancement can be attributed to both the low intrinsic noise of the ExG-OFET platform and its intrinsic signal amplification mechanism, thus confirming the superior sensing performance of the ExG-OFET architecture for potentiometric ion detection.

4. Conclusions

In conclusion, a Ca^{2+} sensor based on a flexible extended gate organic transistor (ExG-OFET) and an ion-selective membrane has been presented. The sensor is able to monitor free calcium variations in real time with low drift currents, good reproducibility and linearity. Moreover, the selectivity of the sensor have been tested against common interferents often co-present in biological fluids, namely sodium, magnesium, glucose and pH variations, thus confirming the applicability of the proposed approach in realistic scenarios.

Interestingly, thanks to the extended gate structure, the device provides intrinsic signal amplification, which allows it to achieve sensitivities as high as 60 mV dec^{-1}, well above the typical values reported for standalone ISEs, and a limit of detection of 1.6 ± 0.3 μM, which is remarkably an order of magnitude lower than the LOD of the sole membrane measured with a standard potentiometric approach.

These aspects, together with the convenient low-cost materials, low-resolution fabrication techniques, and the consolidated method adopted to produce the sensing element, which comprises a biocompatible solid contact and a robust ion-selective interface, make the proposed device a first-of-its-kind solution for the continuous monitoring of Ca^{2+} in relevant biomedical applications.

CRediT authorship contribution statement

F. A. Viola: Writing – original draft, Validation, Methodology, Investigation, Formal analysis, Conceptualization. **D. Hatami:** Methodology, Investigation, Formal analysis, Conceptualization. **F. Mariani:** Writing – review & editing, Methodology, Investigation, Formal analysis, Conceptualization. **I. Gualandi:** Writing – review & editing, Methodology, Investigation, Formal analysis. **F. Terranova:** Investigation. **E. Scavetta:** Writing – review & editing, Supervision, Funding acquisition. **A. Bonfiglio:** Writing – review & editing, Supervision, Funding acquisition. **A. Spanu:** Writing – review & editing, Supervision, Project administration, Funding acquisition, Conceptualization.

Declaration of competing interest

The authors declare that they have no known competing financial interests or personal relationships that could have appeared to influence the work reported in this paper.

Acknowledgement

F. Mariani, I. Gualandi, E. Scavetta, A. Bonfiglio and A. Spanu acknowledge financial support under the National Recovery and Resilience Plan (NRRP), Mission 4, Component 2, Investment 1.1, Call for tender No. 1409 published on 14.9.2022 by the Italian Ministry of University and Research (MUR), funded by the European Union – NextGenerationEU– Project Title ANALYSER – CUP I53D23005640001- Grant Assignment Decree No. 960 adopted on 30/06/2023 by The Italian Ministry of University and Research (MUR).

F. A. Viola acknowledges the financial support of The Italian Ministry for Universities and Research (MUR) - Young Researchers SoE grant – CUP F23C22001020006.

F. A. Viola and A. Bonfiglio acknowledge the financial support of The Italian Ministry of Health - Piano Operativo Salute - Traiettoria 4, project "Hybrid Hub (H2UB): Modelli cellulari e computazionali, micro e nanotecnologie per la personalizzazione di terapie innovative" - CUP F53C22000580001.

The fabrication of the devices was partially carried out at the Biosensors Lab of the University of Cagliari (Dipartimento di Scienze Biomediche, Pad. C - Cittadella Universitaria di Monserrato).

Data availability

Data will be made available on request.

References

[1] J. Anastassopoulou, T. Theophanides, in: D.P. Kessissoglou (Ed.), The Role of Metal Ions in Biological Systems and Medicine BT - Bioinorganic Chemistry: an Inorganic Perspective of Life, Springer Netherlands, Dordrecht, 1995, pp. 209–218, https://doi.org/10.1007/978-94-011-0255-1_17.

[2] C. Bartolucci, E. Passini, J. Hyttinen, M. Paci, S. Severi, Simulation of the effects of extracellular calcium changes leads to a novel computational model of human ventricular action potential with a revised calcium handling, Front. Physiol. 11 (2020) 1–20, https://doi.org/10.3389/fphys.2020.00314.

[3] A.M. Hofer, E.M. Brown, Extracellular calcium sensing and signalling, Nat. Rev. Mol. Cell Biol. 4 (2003) 530–538, https://doi.org/10.1038/nrm1154.

[4] N.I. Hossain, A. Sharma, S. Sonkusale, A wearable and multiplexed electrochemical sensor suite for real-time sweat ionic content and pH monitoring with IoT integration, IEEE Sensors Lett. 7 (2023) 1–4, https://doi.org/10.1109/LSENS.2023.3300827.

[5] M. Brini, T. Calì, D. Ottolini, E. Carafoli, Neuronal calcium signaling: function and dysfunction, Cell Mol. Life Sci. 71 (2014) 2787–2814, https://doi.org/10.1007/s00018-013-1550-7.

[6] J.C. Calderón, P. Bolaños, C. Caputo, The excitation–contraction coupling mechanism in skeletal muscle, Biophys. Rev. 6 (2014) 133–160, https://doi.org/10.1007/s12551-013-0135-x.

[7] M.D. Bootman, T.J. Collins, C.M. Peppiatt, L.S. Prothero, L. MacKenzie, P. De Smet, M. Travers, S.C. Tovey, J.T. Seo, M.J. Berridge, F. Ciccolini, P. Lipp, Calcium signalling—an overview, Semin. Cell Dev. Biol. 12 (2001) 3–10, https://doi.org/10.1006/scdb.2000.0211.

[8] W.T. Clusin, Mechanisms of calcium transient and action potential alternans in cardiac cells and tissues, Am. J. Physiol. Circ. Physiol. 294 (2008) H1–H10, https://doi.org/10.1152/ajpheart.00802.2007.

[9] M. Forsberg, H. Seth, A. Björefeldt, T. Lyckenvik, M. Andersson, P. Wasling, H. Zetterberg, E. Hanse, Ionized calcium in human cerebrospinal fluid and its influence on intrinsic and synaptic excitability of hippocampal pyramidal neurons in the rat, J. Neurochem. 149 (2019) 452–470, https://doi.org/10.1111/jnc.14693.

[10] H. Kroll, S. Bolsover, J. Hsu, S.H. Kim, P.M. Bouloux, Kisspeptin-evoked calcium signals in isolated primary rat gonadotropin- releasing hormone neurones, Neuroendocrinology 93 (2010) 114–120, https://doi.org/10.1159/000321678.

[11] J.P. Morgan, K.G. Morgan, Calcium and cardiovascular function: intracellular calcium levels during contraction and relaxation ofmammalian cardiac and vascular smooth muscle as detected with aequorin, Am. J. Med. 77 (1984) 33–46, https://doi.org/10.1016/S0002-9343(84)80006-6.

[12] C.A. Tate, M.F. Hyek, G.E. Taffet, The role of calcium in the energetics of contracting skeletal muscle, Sport. Med. 12 (1991) 208–217, https://doi.org/10.2165/00007256-199112030-00005.

[13] Ciosek, Ż., Kot, K., Kosik-Bogacka, D., Łanocha-Arendarczyk, N., Rotter, I., 2021. The effects of calcium, Magnesium, Phosphorus, Fluoride, and Lead on Bone Tissue. Biomolecules. https://doi.org/10.3390/biom11040506.

[14] L.B. Baker, A.S. Wolfe, Physiological mechanisms determining eccrine sweat composition, Eur. J. Appl. Physiol. 120 (2020) 719–752, https://doi.org/10.1007/s00421-020-04323-7.

[15] A. Bogdanova, A. Makhro, J. Wang, P. Lipp, L. Kaestner, Calcium in red blood cells—a perilous balance, Int. J. Mol. Sci. (2013), https://doi.org/10.3390/ijms14059848.

[16] D.A. Bushinsky, Contribution of intestine, bone, kidney, and dialysis to extracellular fluid calcium content, Clin. J. Am. Soc. Nephrol. 5 (2010).

[17] J. Fong, A. Khan, Hypocalcemia: updates in diagnosis and management for primary care, Can. Fam. Physician 58 (2012) 158–162.

[18] M.F. Carroll, D.S. Schade, A practical approach to hypercalcemia, Am. Fam. Physician 67 (2003) 1959–1966.

[19] D.A. Goldstein, in: H.K. Walker, W.D. Hall, J.W. Hurst (Eds.), Serum Calcium, 1990. Boston.
[20] F. Criscuolo, M.I.N. Hanitra, I. Taurino, S. Carrara, G.De Micheli, All-solid-state ion-selective electrodes: a tutorial for correct practice, IEEE Sens. J. 21 (2021) 22143–22154, https://doi.org/10.1109/JSEN.2021.3099209.
[21] E. Lindner, B.D. Pendley, A tutorial on the application of ion-selective electrode potentiometry: an analytical method with unique qualities, unexplored opportunities and potential pitfalls; Tutorial, Anal. Chim. Acta 762 (2013) 1–13, https://doi.org/10.1016/j.aca.2012.11.022.
[22] Y. Li, J. Li, W. Qin, Solid-contact polymeric membrane ion-selective electrodes based on electrodeposited NiCo2S4 nanosheet arrays, Talanta 251 (2023) 123797, https://doi.org/10.1016/j.talanta.2022.123797.
[23] H.Y.Y. Nyein, W. Gao, Z. Shahpar, S. Emaminejad, S. Challa, K. Chen, H.M. Fahad, L.C. Tai, H. Ota, R.W. Davis, A. Javey, A wearable electrochemical platform for noninvasive simultaneous monitoring of Ca2+ and pH, ACS. Nano 10 (2016) 7216–7224, https://doi.org/10.1021/acsnano.6b04005.
[24] O. Isildak, I. Yildiz, Highly selective potentiometric determination of nitrate ions using silver bisdiethyldithiocarbamate based membrane electrodes, Electrochim. Acta 459 (2023) 142587, https://doi.org/10.1016/j.electacta.2023.142587.
[25] R. Shiwaku, H. Matsui, K. Nagamine, M. Uematsu, T. Mano, Y. Maruyama, A. Nomura, K. Tsuchiya, K. Hayasaka, Y. Takeda, T. Fukuda, D. Kumaki, S. Tokito, A printed organic amplification system for wearable potentiometric electrochemical sensors, Sci. Rep. 8 (2018) 3922, https://doi.org/10.1038/s41598-018-22265-1.
[26] J. Zhang, M. Rupakula, F. Bellando, E. Garcia Cordero, J. Longo, F. Wildhaber, G. Herment, H. Guérin, A.M. Ionescu, Sweat biomarker sensor incorporating Picowatt, three-dimensional extended metal gate ion sensitive field effect transistors, ACS. Sens. 4 (2019) 2039–2047, https://doi.org/10.1021/acssensors.9b00597.
[27] Z. Chen, N. Zhang, L. Zhuo, B. Tang, Catalytic kinetic methods for photometric or fluorometric determination of heavy metal ions, Microchim. Acta 164 (2009) 311–336, https://doi.org/10.1007/s00604-008-0048-8.
[28] G.M. Fernandes, W.R. Silva, D.N. Barreto, R.S. Lamarca, P.C.F. Lima Gomes, J. Flávio da S Petruci, A.D. Batista, Novel approaches for colorimetric measurements in analytical chemistry – a review, Anal. Chim. Acta 1135 (2020) 187–203, https://doi.org/10.1016/j.aca.2020.07.030.
[29] Y.W. Chang, P.C. Yu, Y.T. Huang, Y.S. Yang, A high-sensitivity CMOS-compatible biosensing system based on absorption photometry, IEEE Sens. J. 9 (2009) 120–127, https://doi.org/10.1109/JSEN.2008.2011079.
[30] S.D. Moss, C.C. Johnson, J. Janata, Hydrogen, calcium, and potassium ion-sensitive FET transducers: a preliminary report, IEEE Trans. Biomed. Eng. BME-25 (1978) 49–54, https://doi.org/10.1109/TBME.1978.326377.
[31] P. Bergveld, Development of an ion-sensitive solid-state device for neurophysiological measurements, IEEE Trans. Biomed. Eng. BME-17 (1970) 70–71, https://doi.org/10.1109/TBME.1970.4502688.
[32] S. Cao, P. Sun, G. Xiao, Q. Tang, X. Sun, H. Zhao, S. Zhao, H. Lu, Z. Yue, ISFET-based sensors for (bio)chemical applications: a review, Electrochem. Sci. Adv. 3 (2023) e2100207, https://doi.org/10.1002/elsa.202100207.
[33] F. Torricelli, D.Z. Adrahtas, Z. Bao, M. Berggren, F. Biscarini, A. Bonfiglio, C. A. Bortolotti, C.D. Frisbie, E. Macchia, G.G. Malliaras, I. McCulloch, M. Moser, T. Q. Nguyen, R.M. Owens, A. Salleo, A. Spanu, L. Torsi, Electrolyte-gated transistors for enhanced performance bioelectronics, Nat. Rev. Methods Prim. 1. (2021), https://doi.org/10.1038/s43586-021-00065-8.
[34] Y. Li, B. Cui, S. Zhang, B. Li, J. Li, S. Liu, Q. Zhao, Ion-selective organic electrochemical transistors: recent progress and challenges, Small. 18 (2022) 2107413, https://doi.org/10.1002/smll.202107413.
[35] A. Moudgil, K. Hou, T. Li, W.L. Leong, Biocompatible solid-state ion-sensitive organic electrochemical transistor for physiological multi-ions sensing, Adv. Mater. Technol. 8 (2023) 2300605, https://doi.org/10.1002/admt.202300605.
[36] H. Sun, J. Gerasimov, M. Berggren, S. Fabiano, N-type organic electrochemical transistors: materials and challenges, J. Mater. Chem. C 6 (2018) 11778–11784, https://doi.org/10.1039/C8TC03185A.
[37] Yao, Y., Huang, W., Chen, J., Wang, G., Chen, H., Zhuang, X., Ying, Y., Ping, J., Marks, T.J., Facchetti, A., 2021. Flexible complementary circuits operating at sub-0.5 V via hybrid organic–inorganic electrolyte-gated transistors. Proc. Natl. Acad. Sci. 118, e2111790118. https://doi.org/10.1073/pnas.2111790118.
[38] M. Demelas, S. Lai, A. Spanu, S. Martinoia, P. Cosseddu, M. Barbaro, A. Bonfiglio, Charge sensing by organic charge-modulated field effect transistors: application to the detection of bio-related effects, J. Mater. Chem. B 1 (2013) 3811–3819, https://doi.org/10.1039/C3TB20237B.
[39] S.P. White, K.D. Dorfman, C.D. Frisbie, Operating and sensing mechanism of electrolyte-gated transistors with floating gates: building a platform for amplified biodetection, J. Phys. Chem. C 120 (2016) 108–117, https://doi.org/10.1021/acs.jpcc.5b10694.
[40] A. Spanu, L. Martines, M. Tedesco, S. Martinoia, A. Bonfiglio, Simultaneous recording of electrical and metabolic activity of cardiac cells in vitro using an organic charge modulated field effect transistor array, Front. Bioeng. Biotechnol. 10 (2022) 1–9, https://doi.org/10.3389/fbioe.2022.945575.
[41] A. Spanu, M.T. Tedesco, L. Martines, S. Martinoia, A. Bonfiglio, An organic neurophysiological tool for neuronal metabolic activity monitoring, APL. Bioeng. 2 (2018) 46105, https://doi.org/10.1063/1.5050170.
[42] M.S. Thomas, D.Z. Adrahtas, C.D. Frisbie, K.D. Dorfman, Modeling of quasi-static floating-gate transistor biosensors, ACS. Sens. 6 (2021) 1910–1917, https://doi.org/10.1021/acssensors.1c00261.
[43] F. Mariani, I. Gualandi, M. Tessarolo, B. Fraboni, E. Scavetta, PEDOT: dye-based, flexible organic electrochemical transistor for highly sensitive PH monitoring, ACS. Appl. Mater. Interfaces. 10 (2018) 22474–22484, https://doi.org/10.1021/acsami.8b04970.
[44] F. Mariani, I. Gualandi, D. Tonelli, F. Decataldo, L. Possanzini, B. Fraboni, E. Scavetta, Design of an electrochemically gated organic semiconductor for pH sensing, Electrochem. commun. 116 (2020) 106763, https://doi.org/10.1016/j.elecom.2020.106763.
[45] F.A. Viola, A. Spanu, P.C. Ricci, A. Bonfiglio, P. Cosseddu, Ultrathin, flexible and multimodal tactile sensors based on organic field-effect transistors, Sci. Rep. 8 (2018) 1–8, https://doi.org/10.1038/s41598-018-26263-1.
[46] F.A. Viola, J. Barsotti, F. Melloni, G. Lanzani, Y.H. Kim, V. Mattoli, M. Caironi, A sub-150-nanometre-thick and ultraconformable solution-processed all-organic transistor, Nat. Commun. 12 (2021) 5842, https://doi.org/10.1038/s41467-021-26120-2.
[47] J. Bobacka, Potential stability of all-solid-state ion-selective electrodes using conducting polymers as ion-to-electron transducers, Anal. Chem. 71 (1999) 4932–4937, https://doi.org/10.1021/ac990497z.
[48] J. Bobacka, A. Ivaska, A. Lewenstam, Potentiometric ion sensors based on conducting polymers, Electroanalysis 15 (2003) 366–374, https://doi.org/10.1002/elan.200390042.
[49] M. Guzinski, J.M. Jarvis, F. Perez, B.D. Pendley, E. Lindner, R. De Marco, G. A. Crespo, R.G. Acres, R. Walker, J. Bishop, PEDOT(PSS) as solid contact for ion-selective electrodes: the influence of the PEDOT(PSS) film thickness on the equilibration times, Anal. Chem. 89 (2017) 3508–3516, https://doi.org/10.1021/acs.analchem.6b04625.
[50] M. Guzinski, J.M. Jarvis, P. D'Orazio, A. Izadyar, B.D. Pendley, E. Lindner, Solid-contact pH sensor without CO2 interference with a superhydrophobic PEDOT-C14 as solid contact: the ultimate "water layer, Test. Anal. Chem. 89 (2017) 8468–8475, https://doi.org/10.1021/acs.analchem.7b02009.
[51] M.M. de Kok, M. Buechel, S.I.E. Vulto, P. van de Weijer, E.A. Meulenkamp, S.H.P. M. de Winter, A.J.G. Mank, H.J.M. Vorstenbosch, C.H.L. Weijtens, V. van Elsbergen, Modification of PEDOT:PSS as hole injection layer in polymer LEDs, Phys. Status Solidi 201 (2004) 1342–1359, https://doi.org/10.1002/pssa.200404338.